Contrib Mineral Petrol (2006) 151: 45–57
DOI 10.1007/s00410-005-0044-5

ORIGINAL PAPER

D. A. Zedgenizov · B. Harte
Edinburgh Ion Microprobe Facility (EIMF)
V. S. Shatsky · A. A. Politov · G. M. Rylov
N. V. Sobolev

Directional chemical variations in diamonds showing octahedral following cuboid growth

Received: 30 July 2004 / Accepted: 19 October 2005 / Published online: 30 November 2005

Abstract A progression from cuboid to octahedral growth has been observed in 16 natural diamonds from Yakutian kimberlites. X-ray and cathodoluminescence topography have revealed that the change in morphology of diamonds with cloudy cuboid cores may occur without mixed-habit growth but via generation of numerous octahedral apices on cuboid surfaces and subsequent gradual transformation into regular octahedral morphology. Nitrogen aggregation in both cuboid and octahedral domains of such diamonds suggests that they have had a long residence time under mantle conditions. Micro-inclusions in the cuboid domains of the diamonds testify to the nucleation and growth of cuboid cores from a hydrous-carbonatitic (oxidized) fluid. The transition from cuboid hummocky growth rich in inclusions to octahedral growth without inclusions may be linked to decreasing supersaturation in the parent fluid. Measurements of $\delta^{13}C$ and N_{ppm} by ion microprobe show that the chemical variations observed between inner cuboid domains and outer octahedral zones commonly have a systematic character and as such they are probably not due to purely kinetic effects. The peripheral octahedral zones are always enriched in ^{13}C in comparison with inner cuboid ones, and the total nitrogen content decreases with the change from cuboid to octahedral growth. The octahedral outer zones show a gradual progressive increase in $\delta^{13}C$, with an overall change of up to 5‰ from the cuboid core ($\delta^{13}C$ usually between −8 and −6‰) to the diamond margin ($\delta^{13}C$ usually between −4 and −2‰). Decreases in $\delta^{13}C$ of this magnitude with a gradual increase in ^{13}C may be attributed to the Rayleigh fractionation operating on a single parent fluid of close to normal mantle $\delta^{13}C$ composition with diamond precipitating by the reduction of carbonatitic fluid in a closed system. However, one sample shows a variation of $\delta^{13}C$ of approximately −17 to −6‰ and therefore suggests a possible change of fluid source composition from one containing subducted crustal organic carbon to one with common mantle carbon.

Communicated by I. Parsons

D. A. Zedgenizov · V. S. Shatsky · G. M. Rylov · N. V. Sobolev
Institute of Mineralogy and Petrography,
pr. ak. Koptyuga 3, 630090 Novosibirsk, Russia

B. Harte (✉)
Grant Institute of Earth Sciences, School of Geosciences,
University of Edinburgh, EH93JW Edinburgh, UK
E-mail: ben.harte@ed.ac.uk
Tel.: +44-131-6508528
Fax: +44-131-6683184

A. A. Politov
Institute of Solid State Chemistry and Mechanochemistry,
Kutateladze 18, 630128 Novosibirsk, Russia

Introduction

Natural diamonds occur with a range of morphological and physical properties (Harrison and Tolansky 1964; Varshavsky 1968; Suzuki and Lang 1976; Orlov 1977; Gurney 1989; Harris 1992; Lang 1992). These morphologies reflect wide variations in the conditions of diamond formation, predominantly in the Earth's mantle, and provide a basis for interpreting the conditions of growth and the post-growth history.

The principal growth morphologies of diamonds are octahedra with smooth faces (including twinned crystals with prominent octahedral faces described as "macles") and cuboid crystals usually with rough surfaces but an overall cubic habit. Different mechanisms of growth and growth rate apply to these two main diamond varieties (Moore and Lang 1972; Sunagawa 1990), and more detailed variations in growth history may be recognized by involving these major categories and by including crystals of mixed (octahedral plus cuboid) habit (Orlov 1977; Welbourn et al. 1989; Lang 1992; Lang et al. 2004). In addition to the difference in growth morphology, it has been suggested that octahedral and cuboid diamonds differ in key features, such as carbon and nitrogen isotope composition; concentration and

aggregation state of nitrogen defects; and inclusion parageneses (e.g. Orlov 1977; Boyd et al. 1987, 1988, 1994; Sobolev 1991; Galimov 1991; Harris 1992; Bulanova 1995; Cartigny et al. 2001). The extent to which growth mechanisms themselves control these chemical variations has been widely debated. In some circumstances, such as where there is a change in inclusion paragenesis, a major change in source compositions is involved. According to the model of diamond genesis proposed by Haggerty (1986), the octahedral and cuboid primary morphological groups of mantle diamonds reflect different P–T–fO_2 conditions of crystallization in the host rocks. Referring to experimental data on the synthesis of diamonds in metal–solvent systems, Haggerty proposed that high-temperature octahedra crystallize under more reducing conditions than low-temperature cuboid morphologies. The influence of changing oxygen fugacity (either reducing or oxidizing) over diamond precipitation in general has been modelled by Deines (1980) and further discussed by other authors (Taylor and Green 1989; Galimov 1991).

In exploring the causes of differences between octahedral and cuboid natural diamonds, and mantle conditions of diamond growth, much interest is attracted to single diamond that shows more than one growth mechanism and switch between octahedral and cuboid portions in the same crystal. There are several observations of natural diamond crystals with mixed-habit growth during which crystallization proceeded simultaneously on octahedral plane faces and on cuboid hummocky surfaces (e.g. Suzuki and Lang 1976; Welbourn et al. 1989; Shatsky et al. 1999; Bulanova et al. 2002; Zedgenizov and Harte 2004). Some diamonds, described as "coated" (Chrenko et al. 1967; Orlov 1977), show an octahedral core together with an inclusion-rich, commonly fibrous, outer zone which has a cuboid external shape. The term cuboid is commonly applied because, although the overall shape is approximately cubic, the outer surfaces are rough rather than smooth cubic crystal faces. Welbourn et al. (1989) have described diamonds with octahedral cores and cuboid external shape in which the outer parts show mixed-habit growth with cuboid sectors rich in micro-inclusions but apparently not fibrous. Considerable variations in $\delta^{13}C$, nitrogen aggregation state and other infrared (IR) spectroscopic properties occur between the core and outer parts of these "coated diamonds" (Chrenko et al. 1967; Swart et al. 1983; Boyd et al. 1987; Welbourn et al. 1989). In many cases it appears that the marked and sharp changes in the physical and chemical characteristics of "coated" stones involve a major change in the composition of the fluid source from which the diamonds grew. In this paper we keep the term "coated diamonds" for stones with octahedral cores and outer coats of roughly cuboid external shape, but it must be emphasized that differences occur within this group of diamonds according to whether or not a fibrous growth structure is evident in the cuboid outer region (Lang 1992; Lang et al. 2004).

A growth sequence distinct to that of coated diamonds is one in which the main sequence is reversed and the progression is from early cuboid (or rough) growth to later octahedral (smooth or layered) growth. Diamonds showing this cuboid to octahedral sequence are far less visually conspicuous than the coated diamonds, because their cuboid inner portions are hidden and usually not so obviously fibrous as in the case of many coated stones. In this paper we examine a suite of diamonds having octahedral growth in their outer parts coupled with cores showing numerous inclusions and a predominantly cuboid overall shape though without the obvious fibrous structure of many coated diamonds. In addition to examining inclusion features and IR characteristics, the diamonds have been studied using the ion microprobe in order to characterize detailed chemical variations during growth of individual diamonds. We evaluate aspects of mantle growth history and the relative influence of factors, such as growth kinetics, Rayleigh fractionation and changing source compositions on the diamonds examined.

Samples

The samples were selected from a collection of diamonds (sieve class −1 + 0.5) from several Siberian kimberlite pipes (Aikhal, nine samples; Internazionalnaya, four samples; Udachnaya, two samples; Mir, one sample) on the basis of having a cloudy central domain, as seen by optical microscopy. Such crystals were most abundant between the Aikhal and Internazionalnaya diamond populations, where they formed 3–5% of a representative collection of more than 1,000 crystals from each pipe. The same type of crystals in the Udachnaya and Mir pipes forms less than 2% of the total population. Sample numbers are given as part of Table 1.

The selected diamonds are predominantly of octahedral external habit, but many of them show some departure from perfectly regular octahedra by the presence of rough surfaces close to {100} and {110} planes. These surfaces are made up of inclined tips and edges of octahedral growth layers. The crystals often have typical resorption features, expressed as the rounding of tops and edges of octahedra and the appearance of triangular etch-pits on {111} faces. To expose the interior of the diamond, the crystals were polished along {110} planes into flat plates 50–70 μm in thickness.

Methods

We have studied the internal structure, carbon isotope composition and nitrogen characteristics of diamonds showing a change in growth morphology from cuboid to octahedral. The internal structure was investigated by imaging of birefringence, X-ray topography, cathodoluminescence (CL) and photoluminescence (PL). Birefringence patterns of polished plates were observed on a

Table 1 FTIR data for diamonds showing octahedral following cuboid growth

Sample	Domain	IaA (ppm)	IaB (ppm)	Total (ppm)	Aggregation state	H (3,107) (cm^{-1})	Fluid-related bands	H_2O/CO_2, molar ratio
A-2	Cuboid	980	1,669	2,649	63	12	1,466, 878, 1,655, ~3,250	0.07
	Octahedral	420	625	1,045	60	1		
A-10	Cuboid	644	527	1,171	45	65	1,453, 883, 1,650, ~3,250	0.06
	Octahedral	330	177	507	35	–		
A-11	Cuboid	1,024	1,884	2,908	65	56	1,435, 879, 1,657, ~3,250	0.11
	Octahedral	308	416	724	58	–		
A-13	Cuboid	708	580	1,288	45	63	1,451, 881, 1,650, ~3,250	0.08
	Octahedral	317	163	480	34	1		
A-16	Cuboid	865	1,194	2,059	58	17	1,454, 879, 1,668, ~3,250	0.09
	Octahedral	358	421	779	54	–		
A-21	Cuboid	814	1,654	2,468	67	13	1,454, 878, 1,657, ~3,250	0.07
	Octahedral	378	702	1,080	65	5		
A-15	Cuboid	936	1,539	2,475	62	25	1,454, 879, 1,655, ~3,250	0.05
	Octahedral	204	229	433	53	1		
A-18	Cuboid	671	1,193	1,864	64	18	1,456, 879, 1,655, ~3,250	0.12
	Octahedral	268	385	653	59	–		
A-12	Cuboid	840	1,260	2,100	60	33	1,452, 881, 1,655, ~3,250	0.08
	Octahedral	414	578	992	58	2		
Mr-02	Cuboid	805	1,496	2,301	65	30	1,458, 881, 862, 1,645, ~3,250	0.14
	Octahedral	418	713	1,131	63	+		
Ud-5	Cuboid	732	853	1,585	54	22	1,456, 881, 862, 1,650, ~3,250	0.14
	Octahedral	347	361	708	51	–		
Ud-03-1	Cuboid	742	517	1,259	41	68	1,454, 883, 863, 1,650, ~3,250	0.08
	Octahedral	275	148	423	35	+		
I-03-1	Cuboid	490	435	925	47	7	1,095, 1,004, 1,454, 883, 1,650, ~3,400	0.36
	Octahedral	232	130	362	36	+		
I-03-2	Cuboid	538	517	1,055	49	14	1,451, 880, 1,650, ~3,250	0.05
	Octahedral	327	246	573	43	–		
I-03-3	Cuboid	495	291	786	37	26	1,095, 1,005, 1,451, 880, 1,650, ~3,400	0.22
	Octahedral	226	71	297	24	–		
I-02	Cuboid	269	76	345	22	8	1,100, 1,004, 1,450, 880, 1,650, ~3,400	0.35
	Octahedral	42	2	44	5	N/D		

Sample localities: A Aikal, Mr Mir, Ud Udachnaya, I Internazionalnaya

Zeiss Axiolab polarized microscope. The X-ray topography on small samples requires some new specifications. Application of a microfocus X-ray source (CuK_α emission) and a long collimator produces a well-focused X-ray beam, and a high resolution of topographic images was achieved in this way. The CL images were obtained by using a JSM-35 scanning electron microscope ($I = 3$ nA, $U = 20$ kV) at the Institute of Mineralogy and Petrography, Novosibirsk, and a Phillips XL30CP scanning electron microscope at the Grant Institute of Earth Sciences, Edinburgh University. The PL topography and spectroscopy of the crystals were performed in Novosibirsk on a universal microscope-spectrophotometer (MSFU-5). The excitation source was the ultraviolet band of a mercury lamp ($\lambda = 313$–365 nm), and the PL spectra were recorded at 77 K with spatial resolution controlled by an aperture set to a minimum value of 20 μm.

The impurity defects and their distribution in the crystals were initially characterized by using IR and luminescence spectroscopy. This enabled determination of nitrogen content, nitrogen aggregation state and the detection of other "organic" (C, O, N, H and S) species (Mendelssohn and Milledge 1995). IR spectra were recorded on an IR Fourier-spectrometer Bruker IFS 66 equipped with a microscope. The aperture of the IR beam was 30 μm and the scan numbers were 100. To correct for scattering of IR radiation, the spectra were baselined interactively. Nitrogen contents and the extent of aggregation were determined by deconvolution of the IR spectral envelope in the 1,350–1,100 cm^{-1} region referenced against the standard IaA–IaB spectra. This involved normalizing the IR spectra to a constant pathlength of 1 mm by setting the absorbance at 1,992 cm^{-1} to 1.23 (Mendelssohn and Milledge 1995). The nitrogen concentration of A and B defects was calculated from the ratios proposed by Woods et al. (1990).

The carbon isotope composition and nitrogen concentration at selected points across the diamonds were measured by using an ion microprobe (SIMS). This technique allows the detailed spatial correlation of these parameters with the detailed growth structure (e.g. Harte et al. 1999; Hauri et al. 2002). In this study nitrogen abundance and C isotope composition in the samples were measured in relation to synthetic standards by using a CAMECA ims-4f ion microprobe, with a Charles Evans and Associates control system for magnetic peak switching, at the NERC Facility in the Grant Institute of Earth Science, School of Geosciences, University of Edinburgh. The general procedures of measurement and estimation of errors are given in detail in

Harte et al. (1999) and Fitzsimons et al. (1999, 2000). However, in the present measurements for carbon (but not nitrogen), energy filtering was applied by using a 300 V offset for carbon. The Cs primary ion beam used in both the cases was 20–30 μm in diameter, but in the case of nitrogen the secondary ion beam was cut to 8 μm by a field aperture.

Results

Internal structure

The topographic study of the polished plates revealed a complex internal structure centred around an inner domain which was usually crowded with numerous tiny inclusions (with sizes of one or several microns) and therefore of cloudy appearance. Such central domains with micro-inclusions typically outline a cuboid shape for the initial crystals as illustrated in Fig. 1. In one of the studied diamonds the central domain showed an intergrowth twin of cuboids. The chains of numerous micro-inclusions in cuboid cores trace octahedral growth directions (Fig. 1b, d). In X-ray topography the central cuboid domains showed a diffraction contrast to the outer octahedral regions (Fig. 2). A dark contrast on transmission X-ray topograms caused by specific dislocations depends on reciprocal orientation of the diffraction vector and the Burgers vector according to invisibility criteria $g \times b = 0$ and $g \times b \times l = 0$, where g is the diffraction vector and b and l are the Burgers vector and line vector, respectively. In the present samples a close dependency of this type was absent and the dark contrast of the cuboid cores was observed at any diffraction vector g; thereby indicating a wide variety of dislocations with different orientations. Overall, the cuboid portions of the present diamonds have high densities of inclusions and dislocations like the cuboid part of coated diamonds, but they lack the strong fibrous features of many coated diamonds.

With PL imagery the central cuboid domain of the studied diamonds shows yellow and greenish-yellow luminescence, whereas the surrounding, essentially octahedral region is characterized by blue and dark-blue luminescence. Occasionally, some PL and CL zonation is apparent within the cuboid central zone. CL imagery shows that the regions immediately surrounding the cuboid central domains are made up of numerous small octahedral apices, which are largely a result of the repetition of small octahedral faces having two main

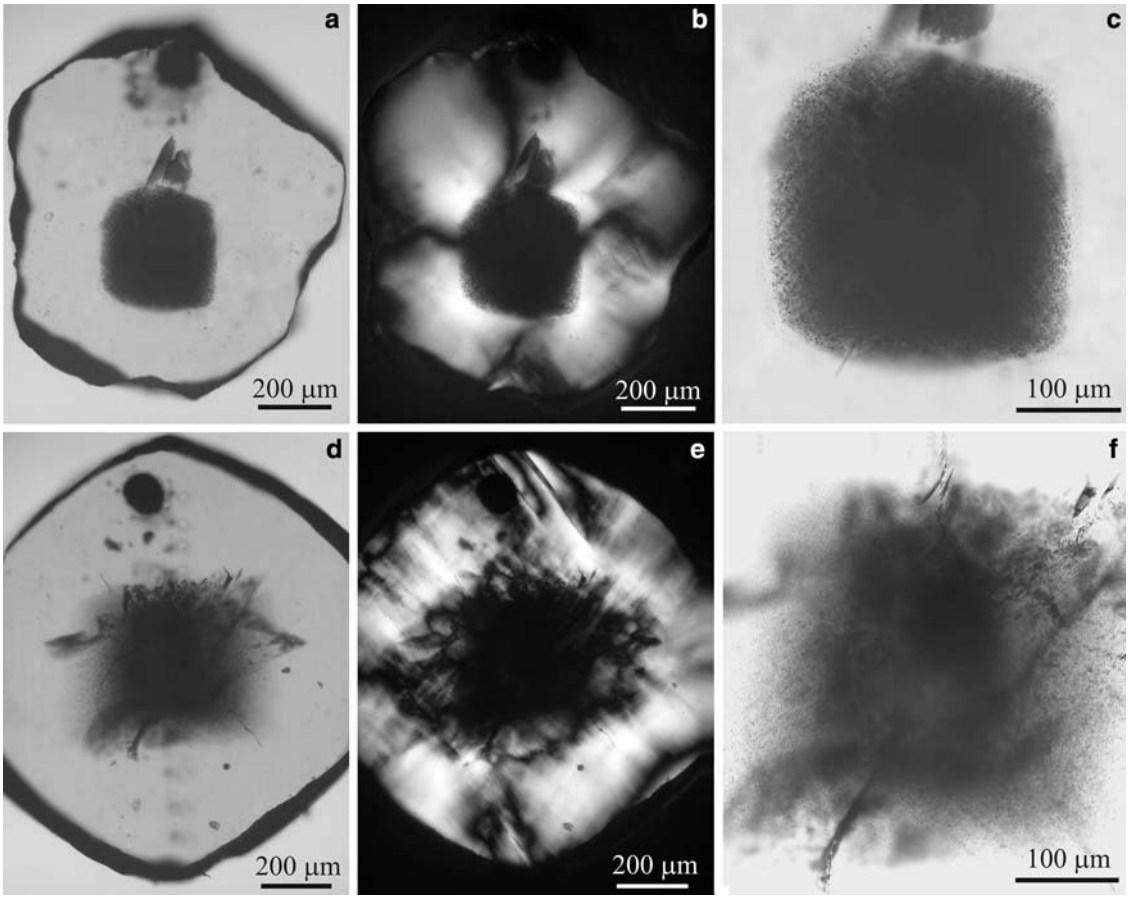

Fig. 1 Transmitted light images (**a** and **d**) and birefringence images (**b** and **e**) of diamonds (I-02-3) and (A-13), respectively, showing their opaque central cuboid cores which contain numerous micro-inclusions. **c** and **f** show the cuboid cores of the same diamonds in more detail

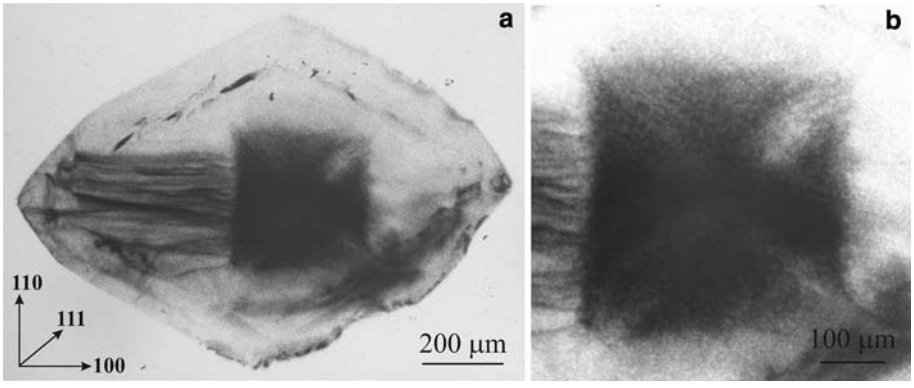

Fig. 2 X-ray topographic images of diamond (Ud-5) with cuboid core and outer octahedral zones. **a** Shows the whole diamond and **b** the cuboid core in detail. The diffraction contrast between cuboid core and the surrounding area is clearly observed. The dark contrast of the cuboid core is due to numerous dislocations with varying orientations (see the text). Cuboid growth sectors are visible in the core. Lines of dislocations propagating from core to the rim in the (100) direction are also seen on the left in the octahedral zone

orientations (Fig. 3). Passing outwards the octahedral faces of the apices tend to increase in size and consolidate, so that there is a gradual transformation to a regular octahedron. Domains of this consolidation are imperfect, so that the diamonds may show many dislocations propagating in the cuboid growth direction (see Fig. 2).

In the early stages of the shape transition, the alternating repetition of differently orientated tiny octahedral faces maintains an overall cuboid shape. Crystals showing similar internal cuboid shapes have been widely described for diamonds from kimberlite and ultra-high-pressure metamorphic rocks (e.g. Shatsky et al. 1998; Zedgenizov et al. 1998; Harte et al. 1999). Many of the studied diamonds are not regular octahedra and different degrees of shape transition may be responsible for the variety of habits of the diamonds (as illustrated by

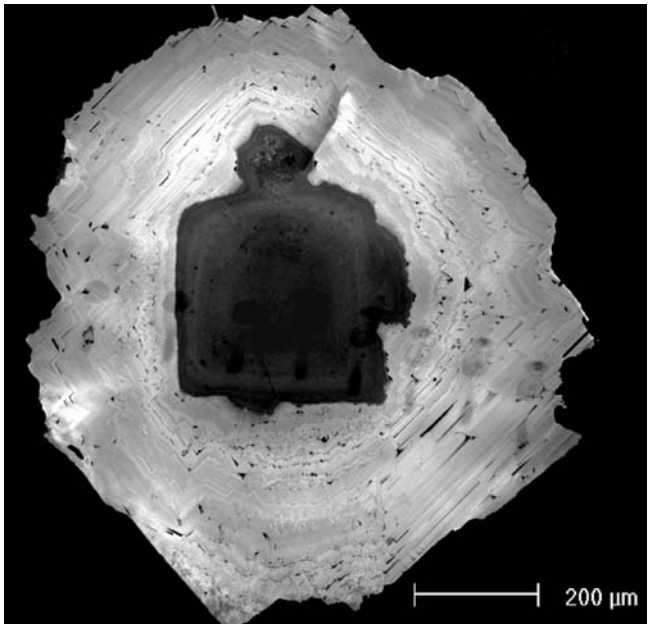

Fig. 3 CL image of polished plate of diamond (A-10). The diamond shows a dark clouded core of dominantly cuboid shape around which is a region of octahedral growth with numerous small octahedral apices (formed by growth on two sets of small octahedral faces which appear in the image to be at approximately 90°). In the outer part the small octahedral faces are seen to become progressively larger and lead to a dominance of few relatively large octahedral faces towards the margin. The small dark areas within the diamond are ones of low CL intensity, and in some cases they reflect the presence of the small octahedral apices by making triangular or arrowhead shapes

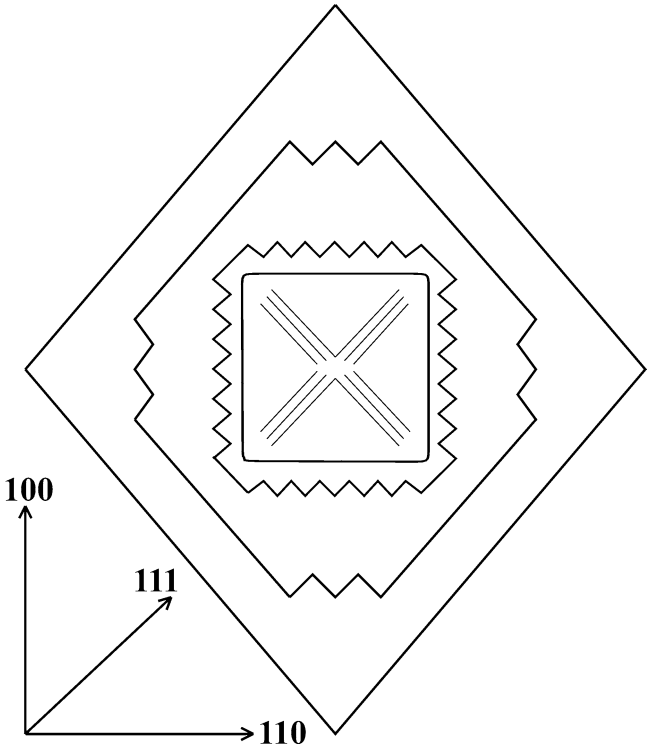

Fig. 4 Idealized scheme of change of shape of natural diamonds from cuboid to octahedral morphology. Following the formation of cuboid core development proceeds by layer-by-layer growth on very small octahedral faces. As further growth proceeds the octahedral faces become progressively larger until a diamond shape dominated by a few large octahedral faces is formed

different stages in Fig. 4). The onset of the transition from cloudy cuboid into octahedral morphology marks an abrupt change in growth mechanism. A similar cuboid to octahedral growth sequence has been shown for a diamond population from the Mir kimberlite pipe (Yakutia) and was described as a case of three-stage growth of natural diamond of octahedral habit (Antonyuk and Mironov 1998). Similar diamonds with a cloudy central zone have recently been described from the Koffiefontein mine (Izraeli et al. 2001), and we presume that such diamonds may be found in many other localities. In this study no evidence was found for mixed-sector growth in which simultaneous growth of cuboid and octahedral face domains occurred (e.g. Bulanova et al. 2002; Zedgenizov and Harte 2004).

Nitrogen content and aggregation state

Nitrogen is known to be the most important structural impurity in diamond and the main types of nitrogen defects have a characteristic absorption in the IR spectrum. The dominant nitrogen defects correspond to spectral types Ib (single nitrogen atoms substituting for carbon atoms), IaA (pairs of nitrogen atoms) and IaB (probably groups of four nitrogen atoms plus a vacancy). The relative abundance of these types reflects the nitrogen aggregation state (e.g. Jones et al. 1992; Mendelssohn and Milledge 1995). Platelet absorption (wavelength $1{,}370 \pm 10$ cm^{-1}) is also usually attributed to nitrogen-related defects, but their structure and composition are not exactly determined.

The diamonds with a central cuboid region studied here have a non-uniform distribution of nitrogen and nitrogen-related defects. Within the cuboid regions the nitrogen content is always higher than in the surrounding octahedral part (Tables 1, 2). In cuboid zones 22–61% of the nitrogen is present as B defects (Table 1). This high degree of aggregation is unlike the cuboid coats of coated diamonds which usually have relatively low degrees of aggregation of nitrogen atoms described as IaA or Ib aggregation states (e.g. Boyd et al. 1988; Shatsky et al. 1999).

The outer octahedral domains in the diamonds of this study have aggregation states that are either similar to or slightly lower than those in the cuboid zones. The observed differences between cuboid and octahedral domains are 300–2,000 ppm in total nitrogen content and 3–17% in aggregation state ($B/(B+A)$). The absorbances due to the B centre and platelets are positively correlated in spectra of both the cuboid cores and the octahedral outer regions, and hence the diamonds belong to the "regular" type of Woods (1986).

Knowledge of the kinetics of nitrogen defect aggregation potentially permits us to estimate the time/temperature history of diamonds (Evans 1992; Taylor et al. 1996; Mendelssohn and Milledge 1995), but the rate of nitrogen aggregation is also proportional to the overall nitrogen abundance. We have found that the content of nitrogen decreases when passing from cuboid to octahedral regions and the degree of aggregation may similarly decrease or remain constant. The high nitrogen aggregation state in both central and peripheral domains of the crystals is a clear evidence of their long-term residence in the mantle. However, the values of time/temperature determined by the second-order kinetic equation (Mendelssohn and Milledge 1995) suggest that

Table 2 SIMS C isotope and N content data: in core to rim sequence for selected diamonds showing octahedral following cuboid growth

Sample	Growth zone	δ^{13}C		N	
		‰PDB	1s (±)[a]	ppm	1s (±)[a]
Ud-03-1	Cuboid	−6.7	0.59	1,410	32
		−7.9	0.59	1,357	64
		−7.1	0.51	1,313	37
	Octahedral	−5.9	0.55	434	19
		−4.7	0.41	399	19
		−3.3	0.35	511	11
		−2.2	0.16	336	33
		−1.8	0.11	417	7
A-10	Cuboid	−5.6	0.44	N/A	N/A
		−5.4	0.34	1,320	58
		−5.6	0.41	1,082	32
	Octahedral	−4.1	0.31	482	27
		−3.3	0.24	528	17
		−3.7	0.29	N/A	N/A
		−4.2	0.34	520	16
A-13	Cuboid	−8.2	0.61	1,002	9
		−7.8	0.46	950	21
		−8.1	0.62	863	15
		−7.5	0.49	1,044	38
		−7.4	0.50	846	23
	Octahedral	−6.3	0.45	459	8
		−5.2	0.30	340	4
		−4.3	0.32	332	6
		−4.4	0.24	230	24
		−4.1	0.31	267	6
		−4.8	0.37	209	7
A-16	Cuboid	−7.0	0.66	N/A	N/A
		−5.1	0.35	N/A	N/A
	Octahedral	−3.3	0.30	N/A	N/A
		−3.2	0.30	N/A	N/A
I-02	Cuboid	−17.1	1.18	312	18
		−15.9	1.03	330	17
		−15.8	1.03	291	16
		−15.3	0.93	N/A	N/A
		−15.0	1.11	N/A	N/A
		−17.4	1.29	N/A	N/A
		−16.4	1.24	207	11
		−15.6	1.03	N/A	N/A
		−14.4	1.14	169	21
	Octahedral	−7.7	0.46	N/A	N/A
		−6.6	0.66	34	2
		−6.3	0.43	27	5
I-03-2	Cuboid	−8.1	0.58	952	15
		−6.8	0.65	879	17
	Octahedral	−4.8	0.36	800	14
		−4.5	0.29	520	8
		−4.0	0.38	617	7
		−3.5	0.37	588	10
		−2.7	0.26	N/A	N/A

[a]Errors are standard errors of the mean for measurements (each of 50 cycles) made on each point

the outer octahedral zones are older than the central zones (Fig. 5). This evident artefact may be due to different activation energies of the transformation of nitrogen centres for cubic and octahedral crystals. Such differences of activation energies have been detected for the C to A transformation in natural and synthetic diamonds (Taylor et al. 1996) and are estimated to be at least 1.5 eV. A second alternative explanation is that the nitrogen aggregation from A- to B-defects is not adequately described by the assumed second-order kinetic equation. For example, Klyuev et al. (1982) considered the transformation of nitrogen defects in synthetic diamonds as a decomposition of oversaturated solid solutions, described by the Avrami equation. However, even in this case, different activation energies are required to explain the variations observed in natural samples. A third possible explanation may be linked to errors in estimation of nitrogen abundance in relation to nitrogen aggregation within thin zones on a scale less than the thickness of the diamond plates transected by the IR beam (Fitzsimons et al. 1999). However, in this case, the total nitrogen contents estimated from FTIR spectroscopy and from SIMS measurements are similar, and marked variations in N abundance are not shown by the SIMS data (Table 2) on octahedral zones.

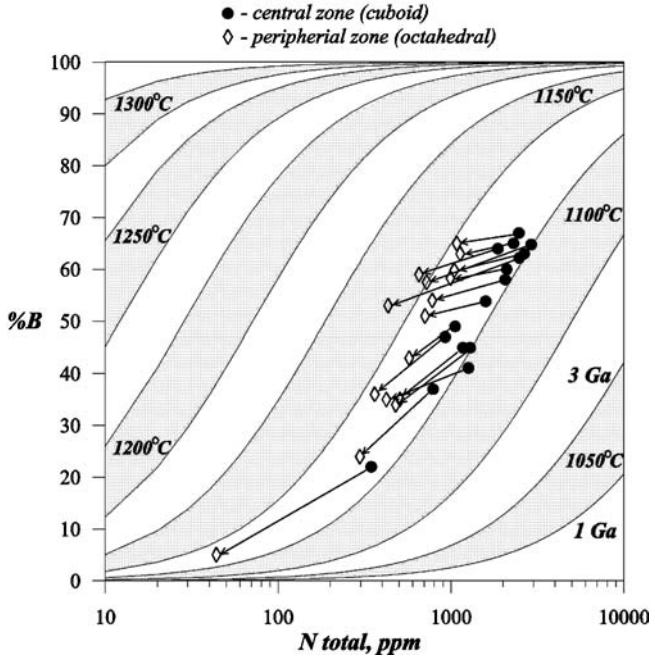

Fig. 5 Nitrogen content (N_{ppm}) versus aggregation state (%B) for cuboid and octahedral domains of individual diamonds (tie lines link data for the same diamond). Theoretical isotherms for different temperatures are shown to illustrate the sensitivity of aggregation state to temperature and mantle residence time as well as N_{ppm}. For each temperature two calculated isotherms are shown; the one above the temperature label is for a mantle residence time of 3Ga, and that below the temperature label is for 1Ga (thus the lines marked 3Ga and 1Ga at the bottom right are for the temperature of 1,050°C). Plot based on that of Taylor et al. (1996)

Hydrogen

A typical feature of the cuboid inner zones is the high intensity of a sharp absorption peak at 3,107 cm^{-1}, which is accompanied by additional less intensive lines at 1,405, 2,786 and 3,227 cm^{-1}. The normalized absorption intensity (Mendelssohn and Milledge 1995) of the peak at 3,107 cm^{-1} in the cloudy cuboid parts varies from 17 to 55 cm^{-1}, whereas in the peripheral octahedral zone (clear from micro-inclusions) the intensity of the peak at 3,107 cm^{-1} does not exceed 5 cm^{-1}. The 3,107 cm^{-1} and associated spectral lines have been attributed to the absorption modes of CH bonds (Chrenko et al. 1967), which may be present as a constituent of the acetylene group CH = CH (Sobolev and Lenskaya 1965) or vinylidene group $>C=CH_2$ (Woods and Collins 1983). It is also proposed that the most likely sites for these groups would be internal surfaces, such as inclusion–matrix interfaces. Thus the evidence of abnormally high intensity of hydrogen absorption in cuboid zones rich in micro-inclusions might be due to localization of hydrogen on the inclusion surfaces (Woods and Collins 1983). In contrast to our inner cuboid regions, the cuboid coats of coated stones do not exhibit such a high hydrogen-related absorption, although they show inclusions. It appears possible that the formation of the H absorption effect in our diamonds is possibly dependent on the occurrence of the high temperature annealing processes which are inferred to give high nitrogen aggregation states compared with coated stones. However, the reasons for the development of the hydrogen peaks clearly require further investigation.

Micro-inclusions

Strong non-diamond contributions to the IR absorption are observed in spectra of the inner cuboid domains, and these may be attributed to the aforementioned abundant micro-inclusions. The IR spectra of the micro-inclusion rich cuboid cores show some features which are obviously similar to those of the cuboid coats of coated diamonds irrespective of the presence or absence of fibrous structure (Chrenko et al. 1967; Navon et al. 1988; Akagi and Matsuda 1988; Schrauder and Navon 1994). Carbonate (1,430 and 878–881 cm^{-1}) and H_2O molecules (3,420 and 1,630 cm^{-1}) are among the principal contributors to the observed IR absorption. The spectra suggest that calcite and the dolomiteankerite series minerals are the most likely candidates for carbonates in the micro-inclusions. Most IR spectra of the cuboid domains also show bands at 575 and 606 cm^{-1}, which can be attributed to phosphate absorption (Navon et al. 1988). In position and shape, these two bands are similar to the doublet of apatite. Apatite has also been found in diamond coats of Siberian diamonds by TEM (Lang and Walmsley 1983). Other bands in the IR spectra of the inclusions include the main silicate bands in the region

between 1,000 and 1,200 cm^{-1}. In samples with high inclusion content silicate absorption bands at 783 and 808 cm^{-1} are observed. These two bands may be attributed to quartz with shifts resulting from high internal pressures preserved in the micro-inclusions (Navon 1991).

From IR spectroscopy we can estimate the amount of the CO_2 component from carbonates as well as water in trapped fluids. Following Navon et al. (1988) the concentration of carbonates and water was calculated using $CO_2 = 213.7 I_{1430}$ ppm and $H_2O = 64.1 I_{3420}$ ppm, where I_{1430} and I_{3420} represent absorption coefficients at 1,430 cm^{-1} for carbonates and 3,420 cm^{-1} for water, respectively. Estimated H_2O/CO_2 molar ratios vary between 0.05 and 0.38, but in general this ratio is less than 0.1 (see Table 1). Three samples from the Internazionalnaya pipe have high H_2O/CO_2 ratios of 0.22–0.38. The observed variations in the composition of micro-inclusions in the cores of the studied samples covers a large part of the range of micro-inclusions in coated cuboid diamonds, which in general lies between carbonatitic and hydrous-silicic endmembers (Schrauder and Navon 1994). Overall, the micro-inclusions in the cuboid cores of the presently studied diamonds are mostly carbonatitic, and therefore indicate a relatively oxidized medium at the time of inclusion formation.

Luminescence data

The heterogeneity of the distribution of defects has been studied in detail for the sample A-11 from the Aikhal kimberlite pipe (see also CL image, Fig. 3). Different growth mechanisms give rise to different centres of luminescence. The central cuboid part shows H4 centres (complex of B defect and vacancy) and N3 centres (complex of three nitrogen atoms plus vacancy). The intensities of these H4 (496.2 nm) and N3 (415.2 nm) centres in different zones of the cuboid core do not correlate with each other. One might also anticipate the occurrence of H3 centres (complex of A defect and two vacancies) in the central part of the diamond, since these are often proportional to the concentration of A defects (Davies and Summergill 1973) which are known to occur in the cuboid regions (see above). However, a careful investigation did not reliably allow us to observe the H3 luminescence. The reason for this may simply be that the position of the main line of the H3 centre (503.2 nm) is close to the position of the line of the H4 centre (503.8 nm); and under strong non-uniform internal stress in the central part of the sample, separate observation of the centres may be extremely difficult.

The peripheral part of diamond A-11 contains mainly N3 centres, which give rise to its strong blue luminescence. No H3 and H4 centres are registered in the peripheral part of the crystal. The estimated concentration of N3 centres in the peripheral part of the diamond is two to ten times higher than that in the central part and its distribution is uniform.

SIMS data—carbon isotope composition

SIMS analyses were made in traverses in the (100) direction across six diamonds (three from Aikhal, two from Internazionalnaya and one from Udachnaya). These traverses were used to compare values of $\delta^{13}C$ and N_{ppm} in growth zones belonging to the different morphologies clearly exhibited by the CL imagery. The SIMS dataset is presented in Table 2.

In all samples variations in the carbon isotope compositions show a broad correlation with the CL zoning structure. Significant variations of $\delta^{13}C$ have been determined with the change of crystal shape from cuboid to octahedral: the cuboid core in individual crystals always has a lighter carbon isotopic composition than the surrounding region of octahedral growth (Table 2). With one exception, the $\delta^{13}C$ values of the inner cuboid domains fall in a narrow range from -5 to $-8‰$, which is similar to but marginally on the higher side of the normal mantle value of ca.$-5‰$ (e.g. Sobolev et al. 1979; Galimov 1991; Cartigny et al. 2001). $\delta^{13}C$ values of -5 to $-8‰$ are also typical of the majority of coated diamonds worldwide (Boyd et al. 1987). However, a marked exception in our dataset is sample (I-02) from the Internazionalnaya kimberlite pipe, which shows $\delta^{13}C$ values in the cuboid core from -14.4 to $-17.4‰$.

As the growth changes from cuboid to octahedral, the values of $\delta^{13}C$ change towards heavier carbon isotope compositions. The overall range of $\delta^{13}C$ in all the octahedral domains is from -1.8 to $-7.7‰$, with the maximum range in any single diamond being 4.1‰.

Two samples Ud-03-1 (range 4‰) and I-03-2 (range 2‰) show a distinct gradual increase of $\delta^{13}C$ towards the rim in the octahedral growth regions. A similar but weaker increase in $\delta^{13}C$ from inner to outer octahedral zone for samples A-13 and I-02 is still above the standard errors of the means (Table 2) and suggests a systematic pattern. In some of the cuboid cores (e.g. A-16 and I-03-2), there is also a suggestion of increasing $\delta^{13}C$ from central to outer cuboid zones. In other cases the cuboid cores show a little variation and no systematic pattern. In general the differences in $\delta^{13}C$ between central cuboid and outermost octahedral domains for individual diamonds lie in the range 2–5‰; excluding the exceptional sample (I-02) with a difference of approximately 10‰.

SIMS data—nitrogen concentration

The SIMS nitrogen data confirm the finding of the FTIR study that the total nitrogen content decreases with the growth change from cuboid to octahedral modes (Tables 1, 2). With the exception of sample I-02, the concentration of nitrogen in cuboid central domains is consistently high at 846–1,410 ppm (Table 2 and Fig. 6), and these variations are within the typical range of those of coated cuboid diamonds (Boyd et al. 1987; Cartigny et al. 2003). Sample I-02 has nitrogen content in its

central cuboid domain of 290–330 ppm; thus, similar to $\delta^{13}C$, the $N_{ppm,}$ falls outside the range of cuboid coats. The nitrogen content in octahedral zones varies from 30 to 800 ppm, but is commonly in the range 200–600 ppm (Table 2 and Fig. 6). The lowest nitrogen concentration has been found in the sample I-02, and this again may indicate a difference to other samples; although, like other samples the concentration of nitrogen drops from cuboid to octahedral growth zones.

Discussion

Growth structure and history

The cuboid interiors of the diamonds studied, with their irregular hummocky surfaces and abundance of micro-inclusions and cavities, clearly show a different mode of growth to that of the external zones with octahedral faces and an absence of abundant inclusions. The distorted structure of the cuboid domains is further expressed by their anomalously high concentrations of hydrogen, which is probably localized on the interfaces between the diamond and its micro-inclusions. The vacancy-bearing H4 defects may be due to dislocations and vacancy chains, and the present results are in agreement with other notions concerning the structure and evolution of defects in diamonds of Ia type (Mainwood 1994). The numerous dislocations and vacancy chains cause a strong deformation of the structure and result in the observed birefringence in optical microscopy and dark contrast in X-ray topography. Once the growth mechanism changes to octahedral, the number of vacancies becomes much less, and the prevailing defects are those with a high molar ratio of nitrogen such as N3.

Sunagawa (1990) has drawn distinctions between various growth types in diamonds and other minerals, and proposed a broad relationship between rough and smooth growth in relation to supersaturation. According to this concept, the cuboid hummocky growth in the initial stages of diamond crystallization reflects a high degree of carbon supersaturation above that of a critical value σ^{**} (see Fig. 7). The abundance of inclusions in the cuboid domains is also considered to reflect high supersaturation. At the later stages of growth, when relatively large and smooth octahedral faces formed, the mode of growth was probably controlled by surface dislocations under conditions of relatively low carbon supersaturation. Such conditions would be below the supersaturation condition σ^{*} of Fig. 7 (after Sunagawa 1990). At intermediate supersaturation hopper crystal growth may occur (Sunagawa 1990). In this case the lowering of supersaturation conditions from inner cuboid to outermost octahedral growth is associated with growth on a multitude of small octahedral faces. This leads to a gradual change in crystal morphology as it proceeds from the formation of numerous octahedral apices on rough surfaces with overall average cuboid orientation, to the formation of progressively larger octahedral faces (Figs. 3, 4, 7).

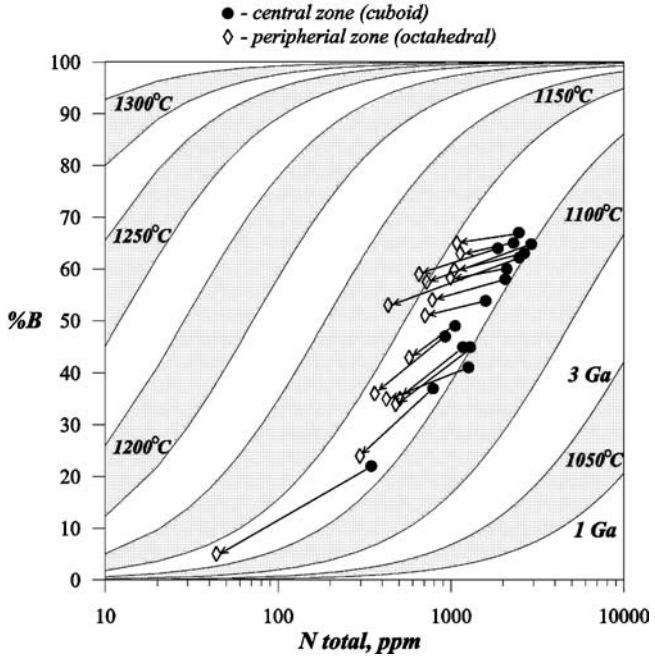

Fig. 6 Carbon isotope and nitrogen abundance trends for diamonds showing octahedral following cuboid growth; solid circular symbols for compositions of cuboid cores; open diamond symbols for outer octahedral regions. Fields for worldwide diamond data from Cartigny et al. (2001) are shown, together with the field of coated diamonds (with cuboid coat on outside of diamond)

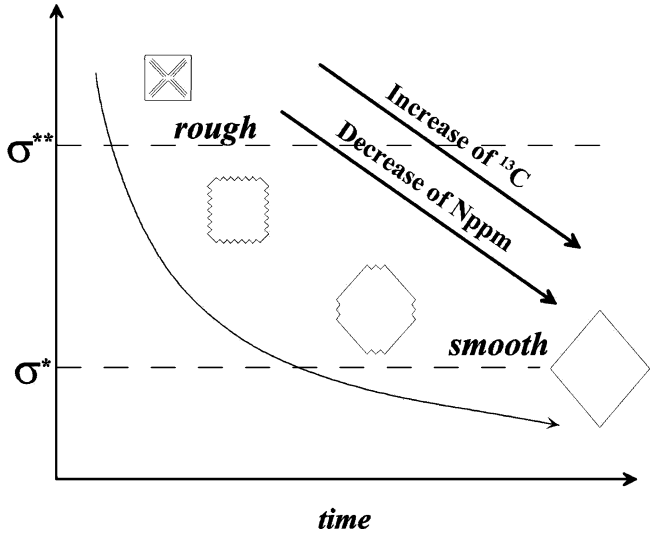

Fig. 7 Schematic drawings showing change of morphology of the diamonds as a function of time and supersaturation (σ). σ^{*} and σ^{**} are critical supersaturation points for different crystal growth types as suggested by Sunagawa (1990): above σ^{**} the solid–liquid interface is rough and continuous or an adhesive-type growth occurs; below σ^{*} the growth forms are polyhedral crystals bounded by flat surfaces, with the crystal growth being principally controlled by interface kinetics and dislocations; at conditions between σ^{*} and σ^{**} hopper crystals are usually expected

Such a progressive decrease in carbon supersaturation during continuous growth may be anticipated under closed-system conditions where growth of the diamond in a limited fluid reservoir would automatically lower carbon concentration in the fluid. If open-system conditions prevailed at the site of diamond growth with fluid infiltration occurring, then the change in supersaturation could be due to a changing composition for the infietrating fluid. The tendency (shown in Table 2 and Fig. 6) for a small downward jump in $\delta^{13}C$ at the time of the cuboid to octahedral transition might be associated with such a change in fluid composition.

The decrease in the abundance of impurities (nitrogen and hydrogen) and lattice defects (vacancy, dislocations and micro-inclusions) when passing from cuboid to octahedral growth may also be linked to differences in growth kinetics for the two diamond types. It is possible that the transition to slower growth may also affect the uptake of nitrogen, because the longer a nitrogen atom is exposed at the growing diamond surface the greater would be the chance of it being displaced by a carbon atom (Boyd et al. 1994). Almost equal levels of nitrogen aggregation at significantly lower nitrogen concentration in the octahedral rims relative to the cuboid centres suggest that the activation energy for the A to B transition may be higher in the cuboid than in the octahedral parts of the diamonds.

The high degree of nitrogen aggregation in the cuboid core domains of the present diamonds suggests long-term residence under mantle conditions. There is clearly a major difference here with the cuboid outer regions of coated diamonds where low nitrogen aggregation states (type IaA or Ib) are observed and argue for a late-stage origin for the cuboid coats (Boyd et al. 1987; Welbourn et al. 1989; Navon 1999). In this case the cuboid cores are an early feature and it appears possible that this factor and their long mantle residence time might also be connected with their lack of obvious fibrous structure. Thus we suggest that the fibrous shapes and coupled markedly elongate structure of micro-inclusions may have existed initially, but have undergone annealing with shape modification at high temperature during the later period of octahedral growth under mantle conditions.

The growth medium—evidence from inclusions

The presence of water and carbonates as micro-inclusions in the core of the studied diamonds provides evidence of their nucleation and crystallization from C–O–H–N fluid. Despite other differences between internal cuboid domains of our diamonds and the cuboid coats of coated stones, the micro-inclusions found in the two types appear to be similar (Lang 1992). The micro-inclusions in fibrous coated diamonds are believed to present either low-density super-critical fluids or volatile-rich melts (Schrauder and Navon 1994; Navon 1999). By analogy with the results of Schrauder and Navon (1994), the strong carbonate absorption in most of our samples suggests the diamond-forming fluid to be carbonate-rich. However, compositions close to a hydrous endmember are observed in several samples from the Internazionalnaya kimberlite pipe.

In general the evidence suggests that nucleation and growth of diamond proceeded either via precipitation of free carbon dissolved in a fluid or through some type of carbonate–silicate interaction probably involving decarbonation. The transition from hummocky cuboid growth to slow octahedral growth is likely to result from a limited supply of supersaturated fluid and may also be linked to a change in the speciation of carbon in the fluid phase. Izraeli et al. (2001) report the occurrence of silicate inclusions in Koffiefontein diamonds with cloudy cores, similar to those studied here. These diamonds belong to both the eclogitic and peridotitic suites, and in both the cases they are associated with micro-inclusions of carbonates and brines. Moreover, the similarity of brine composition in both circumstances led these authors to conclude that diamonds of both suites grew in a single event.

The growth medium—evidence from carbon isotope composition

Carbon isotope composition and nitrogen abundance within diamonds provide other sets of evidence on the following: the chemical composition of the parent fluids, the source of those fluids and their evolution during diamond growth. However, such inferences are by no means clear-cut; with respect to carbon there has been a strong disagreement about the origin of the large isotopic variations involving very low $\delta^{13}C$ values, while for N contents kinetic effects have been suggested (e.g. Deines 1980; Galimov 1984, 1991; Javoy et al. 1986; Boyd et al. 1988, 1994; Kirkley et al. 1991; Cartigny et al. 2001, 2003; Schulze et al. 2003). For nitrogen our observations do not include isotopic data and are limited to N abundance and aggregation state. The large change in N abundance between central cuboid and peripheral octahedral domains might result from a changing fluid composition. But it is notable that the change from cuboid to octahedral morphology is always accompanied by lower N abundance and in the correct direction for a kinetic effect whereby rapidly growing cuboid diamond incorporates an excess of defect atoms while slower growing diamond incorporates less defects and might approach closer to a true equilibrium with the fluid composition (e.g. Boyd et al. 1994; Taylor et al. 1996; Cartigny et al. 2001).

The variations in $\delta^{13}C$ within individual diamonds have been attributed to five major types of factor:

(a) Variations in the source fluid, which reflect heterogeneities in primordial mantle carbon (e.g. Deines 1980; Javoy et al. 1986).
(b) Variations in the source fluid, which include both differences in primordial mantle carbon and carbon

incorporated into the mantle by subduction processes (e.g. Sobolev 1980; Kirkley et al. 1991).

(c) Changing P–T–fO_2 conditions during growth (Deines 1980), which may include outgassing effects (e.g. Javoy et al. 1986).

(d) The Rayleigh fractionation effects between the growing diamond and the fluid source (e.g. Deines 1980). This may be accompanied by isotopic fractionation between basic melt and fluid in the case of eclogitic diamonds (Galimov 1991).

(e) Kinetic effects during crystal growth causing differences in fractionation of carbon and nitrogen for different growth types (e.g. Boyd et al. 1988, 1994).The Rayleigh fractionation between diamond and its parent fluid will occur wherever the fluid reservoir is small enough to have its composition significantly affected by diamond precipitation (i.e. diamond growth in a relatively small closed system) and might accompany any of the other processes (a, b, c, e). Absence of the Rayleigh fractionation and evidence supporting diamond growth from relatively large or continually replenished fluid reservoirs is indicated from detailed ion microprobe studies on several diamonds that show clear growth zonation but little evidence of change in $\delta^{13}C$ (Harte et al. 1999; Hutchison et al. 1999; Kinny et al. 1999).

In this study, the diamonds were selected on the basis of their similarity in growth history and, with one exception, all the diamonds show marked similarities in the nature of their $\delta^{13}C$ variations (Table 2). These similarities are as follows:

1. A general tendency to change from lower $\delta^{13}C$ in the cuboid cores to higher $\delta^{13}C$ in the octahedral rims.
2. Cuboid central zones have constant or slightly outwards increasing $\delta^{13}C$.
3. Octahedral inner zones may show a small difference of plus 1–2‰ relative to the adjacent cuboid material (the I-02 diamond forms an exception with a very large change—see Table 2).
4. Octahedral peripheral zones show a gradual increase in $\delta^{13}C$ usually in the range of 2–4‰.

Boyd et al. (1994) and Cartigny et al. (2001) proposed that for a highly reactive diamond surface and a fluid phase supersaturated with carbon, such as expected for rough cuboid growth, C-bearing species would react to produce new diamond without fractionation between ^{12}C and ^{13}C. In this case, the isotopic composition of the diamond will be controlled only by the isotopic composition of carbon arriving at the growing surface and there will be no difference in the isotopic composition of diamond and fluid. This model may apply to the relatively constant compositions of the central cuboid cores, but it does not provide an explanation for the small increase in $\delta^{13}C$ at the start of octahedral growth. On the basis of the inclusion data, the fluid or melt source from which the diamonds grew was relatively oxidized and CO_2-rich; under this circumstance a decrease in $\delta^{13}C$ would be expected if equilibrium fractionation came into operation at the start of octahedral growth (Bottinga 1969a, b; Deines 1980). A small increase in $\delta^{13}C$ by this fractionation effect would only occur if the fluid was relatively reducing. In the majority of cases the small increase in $\delta^{13}C$ at the time of the change from cuboid to octahedral growth may be linked to a small change in fluid composition and decrease in supersaturation (see above).

Once octahedral growth commences the diamonds show a tendency for $\delta^{13}C$ to gradually increase by about 1–4‰ (Table 2). For a small, closed CO_2-rich fluid reservoir, Deines (1980) calculated that Rayleigh fractionation might lead to an increase in $\delta^{13}C$ in diamond of up to ca.10‰. Kirkley et al. (1991), following the data of Bottinga (1969a, b), suggested that diamond–carbonate fractionations are also relatively large, i.e. −3‰ at mantle temperatures, and can be modelled in a manner similar to the diamond–CO_2 fractionations discussed by Deines (1980). The magnitude of variation of $\delta^{13}C$ from inner to outer parts of the octahedral domains is therefore of a magnitude and direction compatible with a Rayleigh fractionation effect as the diamonds grew from a closed fluid reservoir. The slight tendency to increase in $\delta^{13}C$ seen in the cuboid cores of the diamonds might also be attributed to some Rayleigh fractionation in a partially closed system.

Thus the operation of a consistent set of processes, involving initial cuboid growth at high supersaturation followed by octahedral growth at lower supersaturation and coupled with Rayleigh fractionation from a limited-volume parent fluid, may be applied to most of the studied diamonds. This would explain the variation in carbon isotope compositions as essentially a product of the diamond growth itself without invoking major disequilibrium effects or input of markedly different parent fluids. The exception to this model is diamond I-02 where there is a change of approximately −7‰ in $\delta^{13}C$ between cuboid core and octahedral rim. The magnitude of this jump coupled with the much lighter isotopic composition of carbon (−15 to −17‰) in the cuboid domain compared to the other stones suggests a distinct fluid source for this particular domain. Compared to the other stones the cuboid core of I-02 possibly relates to subducted organic carbon of crustal origin (e.g. Kirkley et al. 1991). Thus in this case the major change in carbon isotopes might result from a change of fluid source from subducted/crustal to asthenospheric/mantle carbon in a similar manner to that described by Schulze et al. (2003, 2004).

Conclusions

We have described natural diamonds with a particular growth history where the crystal morphology progressively changed from cuboid to octahedral. Similar crystals are found in many kimberlite pipes worldwide.

The morphological data show that the change from cuboid habit may occur via generation of numerous octahedral apices on the cuboid surfaces, with a subsequent increase in size of octahedral faces and a gradual transformation to regular octahedral morphology. The nitrogen aggregation state of the diamonds showing octahedral following a cuboid growth suggests that both cuboid and octahedral regions had a long residence time under mantle conditions. The cuboid growth in the interior of the diamonds shows some variations in diffraction contrast to that associated with the cuboid fibrous growth of coated cuboids. It is speculated that these variations partly reflect the difference in annealing time and conditions between the cuboid cores and the late-stage coats of coated cuboid diamonds.

The change of growth morphologies from cuboid to octahedral in the present diamonds is believed to reflect the changing properties of the fluid from which the diamonds grew. The cuboid cores show a multitude of micro-inclusions, and it is suggested that the initial nucleation and growth of the diamonds was from a hydrous-carbonatitic fluid strongly supersaturated in carbon. During the growth of the cuboid cores the diamonds also incorporated a high abundance of N defects. With a fall in supersaturation, the hummocky growth of cuboids was replaced by octahedral face growth on increasingly larger faces towards the margin of the diamonds.

In most cases the initial source fluid probably had $\delta^{13}C$ values of -5 to $-8‰$, close to those expected for normal mantle-derived material. But in one case (diamond I-02) values of -15 to $-17‰$ suggest the possibility of subduction-related, crustal-derived, carbon. In most cases the initial octahedral zones of the diamonds have $\delta^{13}C$ values only slightly displaced from the cuboid cores and a subsequent gradual change of plus 2–4‰ in the $\delta^{13}C$ from the inner to outer octahedral domains is seen. In the case of diamond I-02 there is a sharp jump from -15 to $-7‰$ at the cuboid–octahedral boundary; thereby suggesting input of a new parent fluid with common mantle $\delta^{13}C$ values. However, I-02 also shows a small increase of $\delta^{13}C$ from inner to outer octahedral zones as seen in the other diamonds. The gradual changes in the $\delta^{13}C$ from the inner to outer octahedral domains in all diamonds may be attributed to the Rayleigh fractionation as diamond grew from fluid in a small volume closed system.

Acknowledgements The members of the Edinburgh Ion Microprobe Facility (EIMF) who particularly contributed to this research were Nicola Cayzer (for considerable help with CL imaging of the studied diamonds) and John Craven and Simone Kasemann (for their expertise in tuning the ion microprobe and help in processing of the SIMS data). This work was partially supported by the Russian Foundation for Basic Research (grants 03-05-64040, 01-05-06266 and 04-05-64948) and the UK Natural Environment Research Council (grant F14/G6/40/01). DZ is grateful for a Royal Society/NATO post-doctoral fellowship. Helpful reviews by Jeffrey Harris and Thomas Stachel are gratefully acknowledged.

References

Akagi T, Masuda A (1988) Isotopic and elemental evidence for a relationship between kimberlite and Zaire cubic diamonds. Nature 336:665–667

Antonyuk BP, Mironov VP (1998) Three-stage model of the natural diamond of octahedral habit Ext Abstracts of 7 Inter Kimberlite Conference, pp 23–25

Bottinga Y (1969a) Calculated fractionation factors for carbon and hydrogen isotope exchange in the system calcite-carbon dioxide-graphite-methane-hydrogen-water vapor. Geochim Cosmochim Acta 33:49–64

Bottinga Y (1969b) Carbon isotope fractionation between graphite, diamond and carbon dioxide. Earth Planet Sci Lett 5:301–307

Boyd SR, Pineau F, Javoy M (1994) Modelling the growth of natural diamonds. Chem Geol 116:29–42

Boyd SR, Mattey DP, Pillinger CT, Milledge HJ, Mendelssohn M, Seal M (1987) Multiple growth events during diamond genesis: an integrated study of carbon and nitrogen isotopes and nitrogen aggregation state in coated stones. Earth Planet Sci Lett 86:341–353

Boyd SR, Pillinger CT, Milledge HJ, Mendelssohn MJ, Seal M (1988) Fractionation of nitrogen isotopes in a synthetic diamond of mixed crystal habit. Nature 331:604–607

Bulanova GP (1995) The formation of diamond. J Geochem Explor 53:1–23

Bulanova GP, Pearson DG, Hauri EH, Griffin BJ (2002) Carbon and nitrogen isotope systematics within a sector-growth diamond from the Mir kimberlite, Yakutia. Chem Geol 188:105–123

Cartigny P, Harris JW, Javoy M (2001) Diamond genesis, mantle fractionation and mantle nitrogen content: a study of $\delta^{13}C$–N concentrations in diamonds. Earth Planet Sci Lett 185:85–98

Cartigny P, Harris JW, Taylor A, Davies R, Javoy M (2003) On the possibility of kinetic fractionation of nitrogen isotopes during natural diamond growth. Geochim Cosmochim Acta 67:1571–1576

Chrenko RM, McDonald RS, Darrow KA (1967) Infra-red spectra of diamond coat. Nature 213:474–476

Davies G, Summergill I (1973) Nitrogen dependent optical properties of diamond. Diamond Research, pp 6–15

Deines P (1980) The carbon isotope composition of diamonds: relationship to diamond shape, color, occurrence and vapor composition. Geochim Cosmochim Acta 44:943–961

Evans T (1992) Aggregation of nitrogen in diamond. In: Field JE (ed) The properties of natural and synthetic diamond. Academic, London, pp 259–290

Fitzsimons ICW, Harte B, Chinn IJ, Gurney JJ, Taylor WR (1999) Extreme chemical variation in complex diamonds from George Creek, Colorado: a SIMS study of carbon isotope com-position and nitrogen abundance. Mineral Mag 63:857–878

Fitzsimons ICW, Harte B, Clark RM (2000) SIMS stable isotope measurement: counting statistics and analytical precision. Mineral Mag 64:59–83

Galimov EM (1984) The relation between formation conditions and variations in isotope composition of diamonds. Geokhimiya 8:1091–1118

Galimov EM (1991) Isotope fractionation related to kimberlite magmatism and diamond formation. Geochim Cosmohim Acta 55:1697–1708

Gurney JJ (1989) Diamonds. In: Proceedings of 4th international Kimberlite conference, vol 2. GSA Spec Pub 14:936–965

Haggerty S (1986) Diamond genesis in a multiply-constrained model. Nature 320:34–38

Harris JW (1992) Diamond geology In: Field JE (ed) The properties of natural and synthetic diamond. Academic, London, pp 345–349

Harrison ER, Tolansky S (1964) Growth history of a natural octahedral diamond. Proc R Soc London A279:490–496

Harte B, Fitzsimons ICW, Harris JW, Otter ML (1999) Carbon isotope ratios and nitrogen abundances in relation to

cathodoluminescence characteristics for some diamonds from Kaapvaal Province, SAfrica. Mineral Mag 63:829–856
Hauri EH, Wang J, Pearson DG, Bulanova GP (2002) Microanalysis of $\delta^{13}C$, $\delta^{15}N$ and N abundances in diamonds by secondary ion mass spectrometry (SIMS). Chem Geol 185:149–163
Hutchison MT, Cartigny P, Harris JW (1999) Carbon and nitrogen compositions and physical characteristics of transition zone and lower mantle diamonds from Sao Luiz, Brazil. In: Proceedings of 7th international Kimberlite conference, vol 1 (JB Dawson vol). Red Roof Design, Cape Town, pp 372–382
Izraeli ES, Harris JW, Navon O (2001) Brine inclusions in diamonds: a new upper mantle fluid. Earth Planet Sci Lett 187:323–332
Javoy M, Pineau F, Delorme H (1986) Carbon and nitrogen isotopes in the mantle. Chem Geol 57:41–62
Jones R, Briddon PR, Oeberg S (1992) First-principal theory of nitrogen aggregates in diamond. Phil Mag Lett 66:67–74
Kinny PD, Trautman RL, Griffin BJ, Fitzsimons ICW, Harte B (1999) Carbon isotopic composition of microdiamonds. In: Proceedings of 7th international Kimberlite conference, vol 1 (JB Dawson vol). Red Roof Design, Cape Town, pp 429–436
Kirkley MB, Gurney JJ, Otter ML, Hill SJ, Daniels LR (1991) The application of C isotope measurements to the identification of the sources of C in diamonds. Appl Geochem 6:477–494
Klyuev YuA, Naletov AM, Nepsha VI (1982) Transformation of optically-active centers in synthetic diamonds under the temperature influence (in Russian). J Phys Chem 56:524–531
Lang AR (1992) Diffraction and imaging studies of diamond In: Field JE (ed) The properties of natural and synthetic diamond. Academic, London, pp 215–258
Lang AR, Walmsley JC (1983) Apatite inclusions in natural diamond coat. Phys Chem Mineral 9:6–8
Lang AR, Yelisseyev AP, Pokhilenko NP, Steeds JW, Wotherspoon A (2004) Is dispersed nickel in natural diamonds associated with cuboid growth sectors in diamonds that exhibit a history of mixed-habit growth. J Cryst Growth 263:575–589
Mainwood A (1994) Nitrogen and nitrogen-vacancy complexes and their formation in diamond. Phys Rev B Condens Matter 49:7934–7940
Mendelssohn MJ, Milledge HJ (1995) Geologically significant information from routine analysis of the mid-infrared spectra of diamonds. Inter Geol Rev 37:95–110
Moore M, Lang AR (1972) On the internal structure of natural diamonds of cubic habit. Phil Mag 26:1313–1325
Navon O (1991) Infrared determination of high internal pressures in diamond fluid inclusions. Nature 353:746–748
Navon O (1999) Diamond formation in the Earth's mantle. In: Proceedings of 7th international Kimberlite conference, vol 2 (PH Nixon vol). Red Roof Design, Cape Town, pp 757–763
Navon O, Hutcheon ID, Rossman GR, Wasserburg GJ (1988) Mantle-derived fluids in diamond micro-inclusions. Nature 335:784–789
Orlov YuL (1977) The mineralogy of diamond. Wiley, New York, pp 235
Schulze DJ, Harte B, Valley JW, Brenan JM, Channer DM, De R (2003) Extreme crustal isotope values preserved in coesite in diamond. Nature 423:68–70
Schulze DJ, Harte B, Valley JW, Channer DM, De R (2004) Evidence of subduction and crust mantle mixing from a single diamond. Lithos (in press)
Schrauder M, Navon O (1994) Hydrous and carbonatitic mantle fluids in fibrous diamonds from Jwaneng. Botswana Geochim Cosmochim Acta 52:761–771
Shatsky VS, Rylov GM, Yefimova ES, de Corte K, Sobolev NV (1998) Morphology and real structure of microdiamonds from metamorphic rocks (Kokchetav massif), kimberlites and alluvial placers Geologiya i Geofizika, 39:942–955 (in Russian) English translation: Russ Geol Geophys 39:949–961
Shatsky VS, Zedgenizov DA, Yefimova ES, Rylov GM, Sobolev NV (1999) A comparison of morphology and physical properties of microdiamonds from the mantle and crustal environments. In: Proceedings of 7th international Kimberlite conference, Cape Town, vol 2 (PH Nixon vol), pp 757–763
Sobolev EV, Lenskaya SV (1965) About the occurrence of "gaseous" impurities in spectra of natural diamonds (in Russian). Geologiya i Geofizika 2:157–159
Sobolev EV (1991) The impurity centers and some problems of diamond genesis Ext Abstracts of 5 Inter Kimberlite Conf, Araxa, Brazil, v2, 388–390
Sobolev NV, Galimov EM, Ivanovskaya IN, Yefimova ES (1979) The carbon isotope composition of diamonds containing crystalline inclusions. Dokl Akad Nauk SSSR 249:1217–1220
Sobolev VS, Sobolev NV (1980) New proof on very deep subsidence of eclogitized crustal rocks. Dokl Akad Nauk SSSR 250:683–685
Sunagawa I (1990) Growth and morphology of diamond crystals under stable and metastable conditions. J Cryst Growth 99:1156–1161
Suzuki S, Lang AR (1976) Occurrences of faceted re-entrants on rounded surfaces of natural diamonds. J Cryst Growth 34:29–37
Swart PK, Pillinger CT, Milledge HJ, Seal M (1983) Carbon isotopic variations within individual diamonds. Nature 303:793–795
Taylor WR, Green DH (1989) The role of reduced C–O–H fluids in mantle partial melting. Kimberlites and related rocks, GSA Special Publication, No14, vol 1, pp 592–602
Taylor WR, Canil D, Milledge HJ (1996) Kinetics of Ib to IaA nitrogen aggregation in diamonds. Geochim et Cosmochim Acta 60:4725–4733
Varshavsky AV (1968) Anomalous birefringence and internal morphology of diamond (in Russian). Nauka, Moscow, pp 92
Welbourn CM, Rooney MLT, Evans DJF (1989) A study from diamonds of cube and cube related shape from the Jwaneng mine. J Cryst Growth 94:229–252
Woods GS (1986) Platelets and the infrared absorption of type la diamonds. Proc R Soc London 407:219–238
Woods GS, Collins AT (1983) Infrared absorption spectra of hydrogen complexes in type I diamonds. J Phys Chem Solids 44:471–475
Woods GS, Purser GC, Mtimkulu ASS, Collins AT (1990) The nitrogen content of type Ia natural diamonds. J Phys Chem Solids 51:1191–1197
Zedgenizov DA, Fedorova EN, Shatsky VS (1998) Microdiamonds from Udachnaya kimberlite pipe. Geologiya i Geofizika 39:745–753 (in Russian); English translation in Russian Geol Geophys 39:756–764
Zedgenizov DA, Harte B (2004) Microscale variations of δ13C and N content within a natural diamond with mixed-habit growth. Chem Geol 205:169–175